Journal of Chromatography, 591 (1992) 75–88
Elsevier Science Publishers B.V., Amsterdam

CHROM. 23 767

Physico-chemical properties of electron-acceptor stationary phases in liquid chromatography

Kenneth J. Welch☆ and Norman E. Hoffman*

Chemistry Department, Marquette University, Milwaukee, WI 53233 (USA)

(First received July 30th, 1991; revised manuscript received September 24th, 1991)

ABSTRACT

Some new electron-acceptor (EA) stationary bonded phases (BPs) for liquid chromatography were synthesized and compared with existing EA BPs. The following EA BPs were compared: dinitrophenylmercaptopropylsilica (DNPMP); dinitrodibenzoylmercaptopropylsilica (DNBMP); dinitroanilinopropylsilica (DNAP); dinitrobenzamidopropylsilica (DNBAP); tetranitrofluoreniminopropylsilica (TNFP); tetranitrodibenzosuberiminopropylsilica (TNDBSP); trinitrophenylmercaptopropylsilica (TNPMP); pentafluorophenylsilica (PFPh); aminopropylsilica (NH_2) and Nucleosil 5-NO_2 (5-NO_2). Entropy–enthalpy compensation data indicated that the mechanism of retention (first six BPs) was the same for planar and non-planar aromatic solutes, but it was less informative than the vector-analysis techniques of linear correlation coefficient and Euclidian distance calculations. The latter provided a quantitative comparison of the BPs. All EA BPs had close similarity except for TNFP. NH_2 and 5-NO_2 were similar to the EA BPs. PFPh was not similar to the other EA BPs. The EA BPs were also examined for their ability to group aromatic solutes of similar ring size regardless of alkyl substitution. A new performance parameter, R_r (group resolution), was proposed and applied to these data. Using the calculated values for R_r, the group-resolution effectiveness of the various BP followed the sequence DNAP ≫ DNPMP, TNPMP, 5-NO_2 > TNDBSP, DNBMP, DNBAP > NH_2 > TNFP ≫ PFPh. Retention of aromatic solutes as a function of planarity was also investigated. DNPMP was found to be slightly better than DNAP at separating bridged biphenyls.

INTRODUCTION

Bonding electron-acceptor (EA) groups to silica produces a stationary bonded phase (BP) for effective class separation of polycyclic aromatic hydrocarbons (PAHs) by high-performance liquid chromatography (HPLC). A variety of EA phases have been developed; however, the most common EA phases consist of nitroaromatic molecules bonded to silica via a suitable linking group [1]. Examples of these EA phases include nitrated fluoreniminopropyl [2–5], 2,4-dinitroanilinopropyl [5–12], 2,4-dinitroanilinooctyl [11], picramidopropyl [10–15], picramidooctyl [11], 3,5-dinitrobenzenesulphamidopropyl [10] and 3,5-dinitrobenzamidopropyl [10,16] silicas. The EA phases based on bonded dinitrophenyl or picryl groups have been preferred over the nitrofluorenyl EA phases because they exhibit less peak asymmetry and less selectivity within PAH class types [2,5].

The length of the alkyl group attaching the EA group to the silica surface has had little effect on the grouping of PAH classes [11]. When non-polar solvents are used, the solvophobic electron-acceptor groups remain adsorbed on the silica surface regardless of the size of the linking group.

With EA groups bonded to aminopropylsilica, an acidic hydrogen is available for silanophilic interactions with the surface or for secondary polar interaction with the analyte. The significance of this has not been investigated; however, there are a few EA phases that have been made using linking groups not based on aminopropylsilica: picryl propyl ether-silica [17], dinitrophenylmercaptopropylsilica [18],

☆ Present address: Scientific Support and Government Affairs Division, S. C. Johnson and Son, Inc., Racine, WI 53403-5011, USA.

0021-9673/92/$05.00 © 1992 Elsevier Science Publishers B.V. All rights reserved

dinitrobenzoylmercaptopropylsilica [18] and picrylmercaptopropylsilica [18].

A model for the retention of aromatics on EA phases may be extrapolated from the observations of electron donor–acceptor (or charge-transfer) complexes in solutions [19], in solids [20] and liquid–solid adsorption chromatography (LSC) [21–24]. The retention process consists of displacing sufficient mobile phase molecules to allow the formation of a localized electron donor–acceptor (EDA) complex between a π-electron donor (π-base) solute molecule and a bonded π-electron acceptor (π-acid) group in approximately parallel planes at a short distance (*ca.* 3 Å) [19,20]. An EDA model for chromatography was inferred from the observed correlation between ln k' values (k' = capacity factor) and the first ionization energies for electron-donor molecules. This model was in agreement with the charge-transfer UV spectrum of a solution of anthracene and 2,4-dinitrophenylanilinoethane [9]. Later, a charge-transfer spectrum was observed in the photoacoustic spectrum of anthracene adsorbed on picramidopropylsilica [25]. EDA complex formation is reversible and rapid with a heat of formation of less than 6 kcal/mol [4,8]. The net free-energy change is the sum of the energies of interaction for each group in the donor molecule (*e.g.*, the π electrons [18], aromatic carbons [12] or aromatic rings [11]) with the EA phase less the energy expended to displace the mobile phase molecules. The strength of complex formation is influenced by steric effects. For example, alkylbiphenyls (twelve π-electrons) elute with the same retention time as alkylnaphthalenes (ten π-electrons) instead of with alkylfluorenes (*i.e.*, bridged biphenyls with twelve π-electrons) [18]. Since the acceptor surface may be regarded as planar, the greatest interaction is anticipated with planar donor molecules [21,26,27].

Typically, electron-acceptor phases have been examined with linear free-energy techniques [4,9,10,12,18] or with retention indices [11,28]. The latter technique is well suited for establishing the group-selective aptitude of a particular stationary phase. Two methods used for comparing the retention behaviors of reversed-phase BPs are the extrathermodynamic approaches of enthalpy–entropy compensation [29–38] and homoenergetic–heteroenergetic plots. Neither enthalpy–entropy compensation, derived from techniques used to study solute–solvent interactions [39,40], nor homoenergetic–heteroenergetic plots, used to investigate empirically solute interactions in reversed-phase HPLC [40], have been systematically applied to EA phases.

In this work, we acquired or prepared a variety of EA phases and evaluated them with planar and non-planar solutes. The aim was to compare the various EA phases and observe if certain EA phases had advantages in "grouping", "selecting" or "recognizing" various types of aromatic solutes. The adsorption characteristics of six stationary phases were compared using the techniques of enthalpy–entropy compensation. All stationary phases were compared using vector-analysis techniques and the phases were ranked according to their ability to group alkyl PAHs and recognize planar *versus* non-planar solutes.

EXPERIMENTAL

2,4-Dinitrochlorobenzene, 3,5-dinitrobenzoyl chloride, picryl chloride, pyridine, dibenzosuberone and triethylamine were obtained from Aldrich (Milwaukee, WI, USA). Tetrahydrofuran (THF, "Non-Spectro", Burdick & Jackson Labs., Muskegon, MI, USA) and toluene (Sargent-Welch Scientific, Skokie, IL, USA) were dried over sodium sulphate and sodium metal, respectively, and filtered prior to use. Silica gel (8-μm RoSil, 400 m^2/g) (Alltech, Deerfield, IL, USA) was dried *in vacuo* at 150°C for 3 h. Aminopropylsilica (5-μm RSil, 550 m^2/g) (Alltech) (NH_2 in Fig. 1), Nucleosil 5 NO_2 (Alltech) (5-NO_2 in Fig. 1) and Supelcosil LC-18 octadecyldimethylsilylsilica (Supelco, Bellefonte, PA, USA) (C_{18} in Fig. 1) were used as received.

Mercaptopropylsilica was made, as described previously [17,18], by adding 3.7 g of 3-mercaptopropyltrimethoxysilane (Petrarch Systems, Bristol, PA, USA) to 2.5 g of silica gel and 200 ml of toluene in a reflux apparatus. A mild reflux was maintained for 24 h. The silica was recovered by filtration, washed with toluene, acetone, water and acetone and dried at 60°C *in vacuo*.

Dinitrophenylmercaptopropylsilica (DNPMP in Fig. 1) was prepared by combining 2.5 g of freshly prepared mercaptopropylsilica, 3.0 g of 2,4-dinitrochlorobenzene, 1.2 ml of pyridine and 150 ml of THF in a reflux apparatus [18]. The mixture was allowed to react for 24 h and treated as for

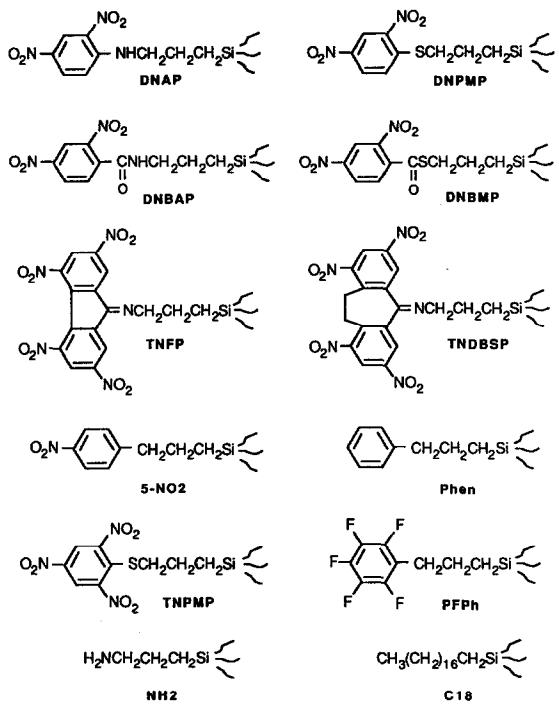

Fig. 1. Various bonded stationary phases used to study the physico-chemical properties of electron-acceptor groups.

mercaptopropylsilica above. Based on elemental analysis (Galbraith Labs., Knoxville, TN, USA), the surface coverage was calculated as 1.12 μmol/m^2.

Dinitrobenzoylmercaptopropylsilica (DNBMP in Fig. 1) and trinitrophenylmercaptopropylsilica (TNPMP in Fig. 1) were prepared by adding 5.2 g of 3,5-dinitrobenzoyl chloride and 3.7 g of picryl chloride to freshly prepared mercaptopropylsilica and completing the steps as for DNPMP above. Based on elemental analyses, the surface coverages were 1.34 and 1.74 μmol/m^2, respectively.

Dinitroanilinopropylsilica (DNAP in Fig. 1) was prepared by combining 3.0 g of 2,4-dinitrochlorobenzene, 2.5 g of 8-μm aminopropylsilica, 1.2 ml of pyridine and 150 ml of THF in a reflux apparatus. After 48 h of refluxing, the mixture was treated as for DNPMP above. Based on elemental analysis, the surface coverage was 1.13 μmol/m^2.

3,5-Dinitrobenzamidopropylsilica (DNBAP in Fig. 1) was prepared [16] by combining 3.5 g of 3,5-dinitrobenzoyl chloride, 2.5 g of 8-μm aminopropylsilica, 2 ml of triethylamine and 150 ml of THF in a septum-sealed reaction flask. The system was stirred and maintained at 60°C. After 24 h, the mixture was treated as for DNPMP above. Based on elemental analysis, the surface coverage was 1.95 μmol/m^2.

2,4,5,7-Tetranitrofluoreniminopropylsilica (TNFP in Fig. 1) was prepared similarly to a procedure described previously [2]. A 2.5-g amount of 8-μm aminopropylsilica was dried by collecting water for 5 h (as the benzene–water azeotrope) with a Dean–Stark moisture trap, 6 g of 2,4,5,7-tetranitro-9-fluorenone were added to the boiling flask and azeotroping was continued for 18 h. The dark-brown silica was collected by filtration and washed with hexane and THF. Based on elemental analysis, the surface coverage was 0.73 μmol/m^2.

The aromatic nitration of dibenzosuberone was performed using the procedure for the nitration of fluorenone [41]. Fuming nitric acid and sulphuric acid (*ca.* 1:1) were slowly added to a refluxing mixture of sulphuric acid (190 ml), fuming nitric acid (325 ml) and 21 g of dibenzosuberone. After 18 h the material was precipitated by pouring the contents into 5 l of cold water. The precipitate was collected by filtration and washed (three times) with hot hexane. Crude product (11 g) was dissolved in a hot solution of 6% acetic anhydride in glacial acetic acid. On cooling, 5.5 g of yellow precipitate with m.p. 197°C recrystallized: ^{1}H NMR ([$^2H_6$]acetone), δ = 8.95 (2H, s), 8.93 (2H, s), 3.72 (4H, s). The nuclear Overhauser effect was observed for ^{13}C nuclei at δ = 128.8 and 123.6. Tetranitrodibenzosuberone was confirmed as the precipitate by direct-probe mass spectrometry (*m/z* 388) and the spot-test for *m*-dinitroaromatics was positive [42]. Based on these data, a structure of 1,3,7,9-tetranitrodibenzosuberone was assigned to this product. 1,3,7,9-Tetranitrodibenzosuberiminopropylsilica (TNDBS in Fig. 1) was made through the same sequence as TNFP. Based on elemental analysis, the surface coverage was 1.48 μmol/m^2.

Pentafluorophenylsilica (PFPh in Fig. 1) and phenylsilica (Phen in Fig. 1) were prepared by adding 3.97 g of pentafluorophenyldimethylchlorosilane and phenyldimethylchlorosilane (Petrarch Systems) to reflux apparatus containing 2.5 g of silica gel, 1.2 ml of pyridine and 150 ml of THF. The mixtures were allowed to react for 24 h and treated as for mercaptopropylsilica above.

The bonded phases were slurry packed with a Micromeritics (Norcross, GA, USA) Model 705 stirred slurry packer at 6000 p.s.i. into 50 × 4.6 mm I.D. stainless-steel columns (Alltech). Each column was installed in an HPLC apparatus consisting of a Waters (Milford, MA, USA) Model 6000A pump with the high-sensitivity pulse damper installed and retrofitted with Model 510 heads, a Rheodyne Model 7125 injector with a 6-μl sample loop, a 2.8-l Equatherm water bath (Curtin Matheson Scientific, Houston, TX, USA), a Vari-Chrom UV-10 variable-wavelength detector (Varian, Sunnyvale, CA, USA), a 300-p.s.i. back-pressure regulator (Alltech) and an SP-4270 printer/plotter (Spectra-Physics, San Jose, CA, USA). Solvent flowing from the pump to the injector passed through a 2-ml stainless-steel loop, immersed in a constant-temperature bath, prior to entering the injector. The columns were evaluated by injecting solutions of various PAHs (*ca.* 200 mg/l) with isooctane (1.0 ml/min) as a mobile phase and monitoring the eluate at 254 nm. Column void volumes were established as the retention time of carbon tetrachloride.

Data analysis was performed with the aid of a VAX 8650 or 6430 computer (Digital Equipment, West Concord, MA, USA) operating the RS1 software package (Bolt Beranek and Newman, Cambridge, MA, USA).

RESULTS AND DISCUSSION

HPLC packings containing a variety of covalently bonded electron-acceptor groups were prepared. 2,4-Dinitroanilinopropylsilica (DNAP) and 3,5-dinitrobenzamidopropylsilica (DNBAP), among the most frequently used EA phases, provided the potential for secondary adsorption owing to the presence of polar hydrogens or a carbonyl group. 2,4-Dinitrophenylmercaptopropylsilica (DNPMP) and 3,5-dinitrobenzoylmercaptopropylsilica (DNBMP) avoided the possibility for secondary adsorption by a polar hydrogen. 2,4,5,7-Tetranitrofluoreniminopropylsilica (TNFP) and 1,3,7,9-tetranitrodibenzosuberiminopropylsilica (TNDBS) provided the possibility of secondary adsorption from an adjacent electron-acceptor ring with planar or non-planar orientation. The capacity factors of various planar and non-planar PAHs were determined over a range of temperatures on each stationary phase using carbon tetrachloride to mark the column volume. Evidence for the "charge-transfer" mechanism in chromatography has generally been regarded as an observed increase in the retention time of aromatic solutes on phases containing electron-withdrawing bonded groups relative to the underivatized stationary phase [13]. This phenomenon has been reported previously for DNAP [8,9], DNPMP [18], DNBAP [10,16], DNBMP [18] and TNFP [2], and was observed for all of the EA phases.

As the EDA complex is reversible, the capacity factor (k') would be proportional to the equilibrium constant (eqn. 1) for the complex and the Van 't Hoff equation (eqn. 3) would apply:

$$k' = K\phi \tag{1}$$

$$\ln k' = \ln K + \ln \phi = -\Delta G^0/RT + \ln \phi \tag{2}$$

$$\ln k' = -\Delta H^0/RT + \Delta S^0/R + \ln \phi \tag{3}$$

where ΔH^0 and ΔS^0 are the standard-state enthalpy and entropy for transfer of the solute molecule from the mobile phase to the stationary phase, R is the gas constant, T is the absolute temperature and ϕ is the phase ratio of the column [29]. A plot of $\ln k'$ *vs.* $1/T$ would yield a straight line (*i.e.*, constant enthalpy) if there is no change in the mechanism or structure of the complex. As Melander *et al.* [29] have demonstrated, when enthalpy–entropy compensation is observed for a family of solutes or stationary phases, the following equation applies:

$$\ln k'(T) = (-\Delta H^0/R)(1/T - 1/\beta) - \Delta G^0_\beta/R_\beta + \ln \phi \tag{4}$$

where $\ln k'(T)$ is the capacity factor for a solute at a particular temperature T, ΔH^0 is the enthalpy of adsorption of the solute and ΔG^0_β is the Gibbs free energy for the adsorption at the compensation temperature β. It is possible to obtain β from a plot of $\ln k'$ *vs.* ΔH^0 for a family of solutes on a stationary phase. If values of β for different chromatographic systems agree (such as within a 95% confidence interval), the retention mechanisms are considered to be the same (or isokinetic).

Linear Van 't Hoff plots have a rigorous thermodynamic basis in the absence of heat-capacity effects. If the mechanism of a process is invariant (*i.e.*, constant enthalpy) over the chosen temperature range, a Van 't Hoff plot yields a straight line. The

Van 't Hoff plots for various EA phases were plotted, and linear regressions ($\ln k'$ *vs.* $1/T$) for the solutes on each EA phase were calculated. With this information, the enthalpies of adsorption were calculated using eqn. 3. These data are summarized in Table I. Applying eqn. 4, the $\ln k'$ values at 45°C for each analyte were plotted against their calculated enthalpies of adsorption on each stationary phase

TABLE I

STATISTICS FROM THE VAN 'T HOFF PLOTS OF VARIOUS ELECTRON-ACCEPTOR STATIONARY PHASES

The columns contain the slope, intercept (Int.), their standard deviations (S.D.) and the coefficient of determination (r^2) calculated for each analyte. The enthalpy and its standard deviation were calculated from the slope data. The mean $\ln k'$ is the logarithm of the capacity factor at the mean temperature of 45°C.

Compound	Column	Slope	S.D. (slope)	Int.	S.D. (Int.)	r^2	ΔH (kcal mol^{-1})	S.D. (ΔH)	Mean $\ln k'$
Benzene	DNAP	826.4	143.4	−3.4	0.4	0.917	1.64	0.28	−0.841
Naphthalene		915.5	107.0	−2.5	0.3	0.961	1.82	0.21	0.399
Anthracene		2060.3	605.1	−4.7	2.1	0.794	4.09	1.20	1.590
Phenanthrene		1779.8	505.5	−3.9	1.7	0.805	3.54	1.00	1.565
Pyrene		1915.6	72.9	−3.7	0.2	0.996	3.81	0.14	2.333
Fluoranthene		1846.9	49.4	−3.4	0.1	0.998	3.67	0.10	2.435
Chrysene		2533.0	65.7	−4.6	0.2	0.998	5.03	0.13	3.408
Fluorene		1245.9	54.8	−2.8	0.1	0.994	2.48	0.11	1.186
Dihydrophenanthrene		977.1	59.2	−2.2	0.1	0.989	1.94	0.12	0.928
Dibenzosuberane		921.8	79.1	−2.0	0.2	0.978	1.83	0.16	0.904
Biphenyl		1355.2	469.7	−3.8	1.4	0.735	2.69	0.93	0.546
Benzene	DNBAP	614.2	356.7	−3.6	1.1	0.497	1.22	0.71	−1.705
Naphthalene		1482.0	208.9	−4.5	0.7	0.944	2.94	0.42	0.148
Anthracene		2185.2	248.4	−5.2	0.9	0.963	4.34	0.49	1.654
Phenanthrene		1946.1	191.3	−4.4	0.7	0.972	3.87	0.38	1.675
Pyrene		2121.8	168.5	−4.3	0.6	0.981	4.22	0.33	2.323
Fluoranthene		2127.4	153.7	−4.4	0.6	0.985	4.23	0.31	2.296
Chrysene		2818.2	316.2	−5.8	1.1	0.964	5.60	0.63	2.998
Fluorene		1869.6	215.3	−5.0	0.8	0.962	3.71	0.43	0.821
Dihydrophenanthrene		1730.2	203.5	−5.1	2.9	0.960	3.44	0.40	0.343
Dibenzosuberane		1641.8	167.8	−4.8	0.6	0.970	3.26	0.33	0.327
Biphenyl		1486.8	224.8	−4.7	0.7	0.936	2.95	0.45	−0.071
Benzene	DNPMP	265.6	84.4	−2.0	0.2	0.767	0.53	0.17	−1.221
Naphthalene		915.5	107.0	−2.5	0.3	0.961	1.82	0.21	0.399
Anthracene		1657.2	81.0	−3.4	0.2	0.993	3.29	0.16	1.882
Phenanthrene		1712.3	72.8	−3.6	0.2	0.995	3.40	0.14	1.824
Pyrene		1915.6	72.9	−3.7	0.2	0.996	3.81	0.14	2.333
Fluoranthene		1846.9	49.4	−3.4	0.1	0.998	3.67	0.10	2.435
Chrysene		2533.0	65.7	−4.6	0.2	0.998	5.03	0.13	3.408
Fluorene		1245.9	54.8	−2.8	0.1	0.994	2.48	0.11	1.186
Dihydrophenanthrene		977.1	59.2	−2.2	0.1	0.989	1.94	0.12	0.928
Dibenzosuberane		921.8	79.1	−2.0	0.2	0.978	1.83	0.16	0.904
Biphenyl		915.7	157.0	−3.0	0.5	0.919	1.82	0.31	−0.094
Benzene	DNBMP	92.4	317.4	−2.4	1.0	0.027	0.18	0.63	−2.004
Naphthalene		773.7	163.7	−3.1	0.5	0.882	1.54	0.33	−0.592
Anthracene		1499.9	95.8	−4.1	0.3	0.988	2.98	0.19	0.646
Phenanthrene		1538.5	96.7	−4.2	0.3	0.988	3.06	0.19	0.697
Pyrene		1707.6	70.6	−4.3	0.2	0.995	3.39	0.14	1.084
Fluoranthene		1751.5	75.4	−4.4	0.2	0.994	3.48	0.15	1.140
Chrysene		2045.7	64.5	−4.7	0.2	0.997	4.06	0.13	1.752
Fluorene		1062.3	87.7	−3.3	0.2	0.980	2.11	0.17	0.082

(Continued on p. 80)

TABLE I *(continued)*

Compound	Column	Slope	S.D. (slope)	Int.	S.D. (Int.)	r^2	ΔH (kcal mol^{-1})	S.D. (ΔH)	Mean ln k'
Dihydrophenanthrene		936.2	117.5	−3.1	0.3	0.955	1.86	0.23	−0.066
Dibenzosuberane		1014.3	132.2	−3.3	0.4	0.952	2.02	0.26	−0.022
Biphenyl		881.7	133.4	−3.3	0.4	0.936	1.75	0.27	−0.449
Benzene	TNFP	677.4	51.8	−3.2	0.1	0.983	1.35	0.10	−1.053
Naphthalene		1180.6	162.1	−3.5	0.5	0.946	2.35	0.32	0.280
Anthracene		2271.3	254.5	−5.1	0.7	0.964	4.51	0.51	2.137
Phenanthrene		1325.7	136.8	−2.4	0.4	0.969	2.63	0.27	1.710
Pyrene		2044.7	139.1	−4.3	0.4	0.986	4.06	0.28	2.083
Fluoranthene		2186.9	128.2	−4.6	0.4	0.990	4.35	0.25	2.294
Chrysene		2583.9	181.2	−4.4	0.6	0.985	5.13	0.36	3.650
Fluorene		2217.1	120.4	−5.8	0.3	0.991	4.41	0.24	1.227
Dihydrophenanthrene		1990.6	274.0	−5.5	0.8	0.946	3.96	0.54	0.750
Dibenzosuberane		1731.6	462.4	−4.7	1.5	0.824	3.44	0.92	0.722
Biphenyl		1151.9	284.3	−3.3	0.9	0.846	2.29	0.56	0.302
Benzene	TNDBSP	434.0	105.9	−3.6	0.3	0.848	0.86	0.21	−2.186
Naphthalene		1208.2	113.7	−4.1	0.3	0.974	2.40	0.23	−0.248
Anthracene		2158.9	29.0	−5.3	0.0	0.999	4.29	0.06	1.523
Phenanthrene		2040.1	155.9	−5.1	0.4	0.983	4.05	0.31	1.343
Pyrene		2163.2	72.0	−4.9	0.1	0.997	4.30	0.14	1.960
Fluoranthene		2318.8	66.5	−5.2	0.2	0.998	4.61	0.13	2.104
Chrysene		3048.8	11.9	−6.4	0.1	1.000	6.06	0.02	3.143
Fluorene		1688.8	96.4	−4.7	0.2	0.990	3.36	0.19	0.604
Dihydrophenanthrene		1516.9	91.9	−4.8	0.2	0.989	3.01	0.18	0.024
Dibenzosuberane		1349.0	121.5	−4.2	0.3	0.976	2.68	0.24	0.024
Biphenyl		1249.4	75.4	−4.3	0.2	0.989	2.48	0.15	−0.418

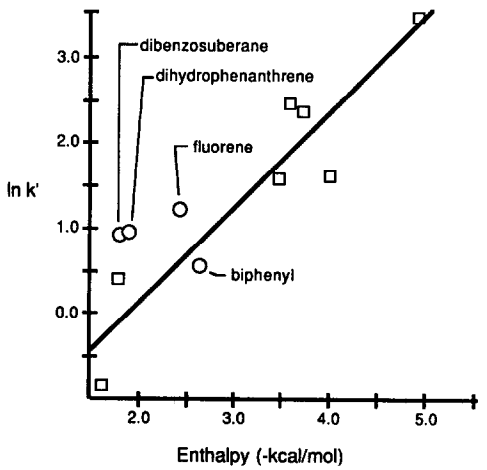

Fig. 2. Entropy–enthalpy compensation plot for (□) planar and (○) non-planar aromatic solutes on dinitroanilinopropylsilica (DNAP).

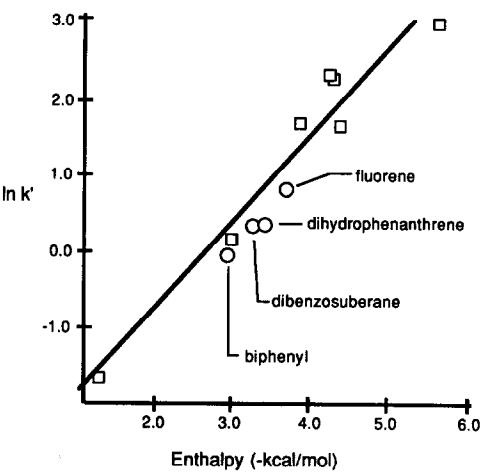

Fig. 3. Entropy–enthalpy compensation plot for (□) planar and (○) non-planar aromatic solutes on dinitrobenzamidopropylsilica (DNBAP).

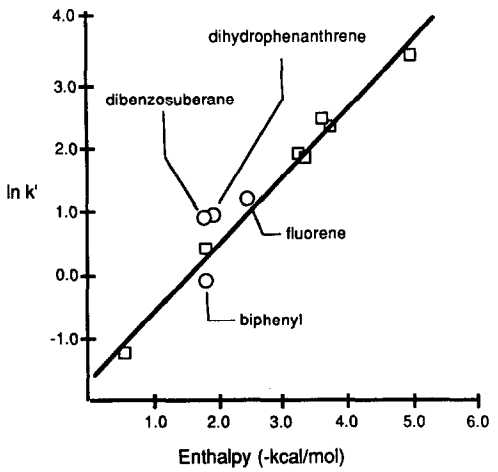

Fig. 4. Entropy–enthalpy compensation plot for (□) planar and (○) non-planar aromatic solutes on dinitrophenylmercaptopropylsilica (DNPMP).

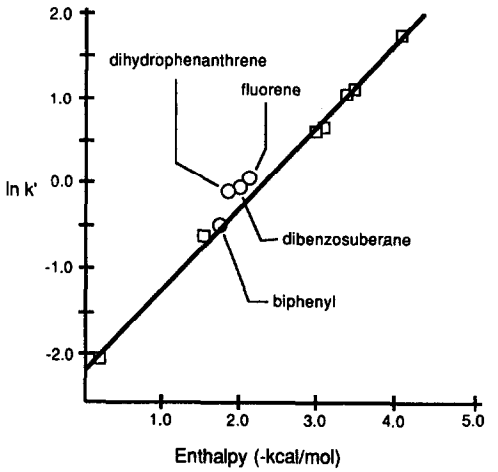

Fig. 5. Entropy–enthalpy compensation plot for (□) planar and (○) non-planar aromatic solutes on dinitrobenzoylmercaptopropylsilica (DNBMP).

(Figs. 2–7). The uncertainties in the enthalpy values were calculated from the uncertainties in the slopes of the Van 't Hoff plots. Compensation of an enthalpy change, produced from an outside stress (such as temperature), by an entropy change is a common occurrence in systems involving small molecules. Common mechanisms are characterized by having $\delta\Delta H$ proportional to $\delta\Delta S$, where δ denotes a change in the thermodynamic parameter caused by a difference in solute, mobile phase or stationary phase. For the various EA stationary phases (Figs. 2–7), the linear locus of data points for the planar compounds indicates consistent enthalpy–entropy compensation, and that the mechanism of adsorption under these conditions was the same for benzene through chrysene. DNAP (Fig. 2), DNBAP (Fig. 3) and TNFP (Fig. 6) had a greater scatter in this linear distribution, as observed from the plots of ln k' *vs.* enthalpy and the standard deviations for the slopes calculated during the linear regression

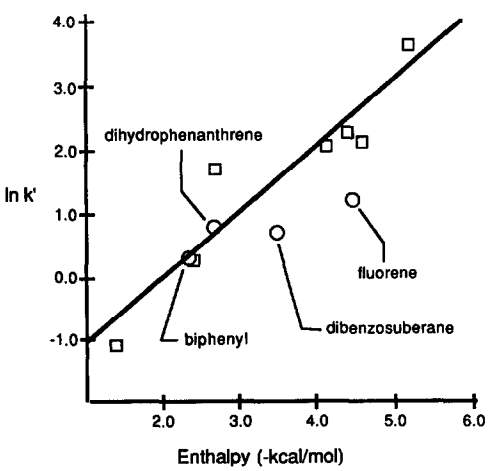

Fig. 6. Entropy–enthalpy compensation plot for (□) planar and (○) non-planar aromatic solutes on tetranitrofluorenimino-propylsilica (TNFP).

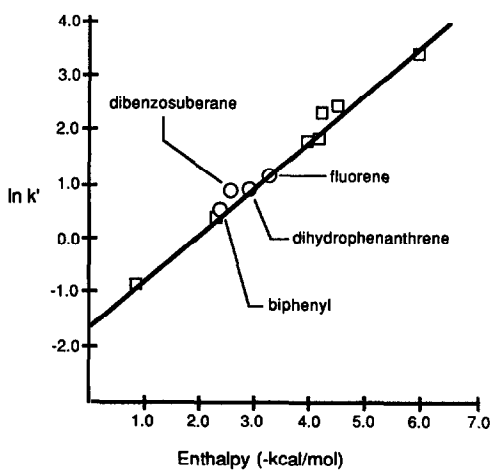

Fig. 7. Entropy–enthalpy compensation plot for (□) planar and (○) non-planar aromatic solutes on tetranitrodibenzosuberiminopropylsilica (TNDBSP).

(Table II). These observations, although reproducible, cannot be explained in terms of the thermodynamic parameters that were evaluated.

The non-planar aromatics (fluorene is grouped with the non-planar compounds for this discussion), had approximately (*i.e.*, within 95% confidence level) the same mechanism for adsorption of the planar solutes. The TNDBS stationary phase was prepared in an attempt to optimize the retention of non-planar aromatics (in particular its dibenzosuberane counterpart). Apparently the sublimity of this stationary phase was ignored by the non-planar solutes in favor of random multi-site orientations which resulted in adsorption behavior similar to those of the other phases. This may be additional indirect evidence for the Monte Carlo model of EDA adsorption [12,43].

If the compensation temperatures (β) are identical for species in different chemical processes, they are believed to share a common physico-chemical property. In this case, similar compensation temperatures for the adsorption of planar aromatic hydrocarbons on different electron-acceptor phases would suggest a common adsorption mechanism among the various phases. Using the recommendations of Krug *et al.* [44,45], compensation temperatures were calculated (Table II) and compared. The compensation temperature of TNDBSP differed from those of DNBAP and DNPMP (>95% confidence level). This suggests that the mechanism of retaining planar solutes may be different on TNDBSP than on either DNBAP and DNPMP. This observation would have been more encouraging had a difference in

TABLE II

ENTROPY–ENTHALPY COMPENSATION IN ELECTRON-ACCEPTOR STATIONARY PHASES

The slope and standard deviation were obtained from the linear regression for the planar solutes. The compensation temperature and the 95% confidence level were calculated from the slope data. The harmonic mean temperature was 318 ± 20 K (95% C.L.).

Stationary phase	Slope of entropy–enthalpy compensation plot (planar)	*n*	Compensation temperature (95% C.L.)
DNAP	1.07 ± 0.18	7	985 ± 426
DNBAP	1.14 ± 0.12	7	1142 ± 309
DNPMP	1.04 ± 0.05	7	931 ± 115
DNBMP	0.95 ± 0.02	7	798 ± 43
TNFP	1.04 ± 0.17	7	930 ± 391
TNDBSP	0.84 ± 0.04	7	679 ± 83

TABLE III

LN *k'* VALUES FOR AROMATIC SOLUTES ON VARIOUS STATIONARY PHASES

No. of π-electrons	Compound	ln *k'*				
		DNAP	DNPMP	TNPMP	5-NO_2	TNDBSP
6	Benzene	−1.825	−1.147	−1.221	−1.551	−2.361
	Toluene	−1.825	−1.099	−1.166	−1.551	−2.179
	o-Xylene	−1.729	−1.147	−1.338	−1.625	−1.891
	Mesitylene	−1.930	−1.371	−1.472	−1.992	−2.179
	Tetralin	−1.562	−1.199	−1.066	−1.551	−1.668
10	Naphthalene	−0.138	0.251	0.180	−0.452	−0.142
	1-Methylnaphthalene	−0.120	0.346	0.284	−0.428	0.000
	1-Ethylnaphthalene	−0.235	0.214	0.152	−0.452	−0.164
	1,5-Dimethylnaphthalene	−0.050	0.492	0.378	−0.361	0.055
14	Anthracene	1.349	2.095	1.697	0.773	1.847
	Phenanthrene	1.354	2.077	1.676	0.794	1.624
	2-Methylanthracene	1.406	2.280	1.767	0.752	2.107
	9,10-Dimethylanthracene	1.587	2.508	1.994	0.834	2.438
	3,6-Dimethylphenanthrene	1.529	2.472	1.927	0.879	2.228
	2-Methylphenanthrene	1.441	2.298	1.767	0.834	1.823
	2-Ethylanthracene	1.302	2.079	1.593	0.693	1.859

mechanism for planar and non-planar solutes been observed for TNDBSP. The compensation temperature treatment may be detecting that TNDBSP has the bulkiest electron-acceptor surface among the EA phases. Similar compensation temperatures were observed for the remaining EA phases (>95% confidence level), indicating a common adsorption mechanism. The compensation temperatures observed for the EA phases (679–1142 K) were slightly higher than those reported for reversed-phase stationary phases (360–897 K) [29,30].

Another extrathermodynamic approach to studying reversed-phase stationary phases is the vector-analysis approach called homoenergetic–heteroenergetic plots [46]. As shown in eqn. 2, the retention of an analyte on a column depends on the phase ratio and the Gibbs free energy for the adsorption process. Consider the retention of an analyte on two different stationary phases at the same temperature:

$$\ln k'_A = -\Delta G^0_A/RT + \ln \phi_A \quad (5)$$

$$\ln k'_B = -\Delta G^0_B/RT + \ln \phi_B \quad (6)$$

If the Gibbs energies for two stationary phases are proportional so that

$$\Delta G^0_A = \rho \Delta G^0_B$$

then eqns. 5 and 6 can be combined to yield

$$-RT(\ln k'_A - \ln \phi_A) = -RT\rho(\ln k'_B - \ln \phi_B) \quad (7)$$

Eqn. 7, with some rearrangement, becomes

$$\ln k'_A = \rho \ln k'_B + \ln \phi_A - \rho \ln \phi_B \quad (8)$$

Capacity factors ($\ln k'$) for a set of analytes (i) on a stationary phase (A) *versus* the $\ln k'$ values for the same analytes on a different stationary phase (B) are vectors that can be used to examine the similarity of A and B. Melander *et al.* [46] stated that when ρ_i/ρ_{i+1} is 1 (*i.e.*, a linear correlation coefficient $\geqslant 0.95$), the phases are homoenergetic (homo = same), and if ρ_i/ρ_{i+1} is not equal to 1 (*i.e.*, a linear correlation coefficient $\leqslant 0.95$), the phases are homeoenergetic (homeo = similar).

The linear correlation coefficient (r) is not unique to homoenergetic–heteroenergetic plots, and is one of the ways to examine similarity between sets of data:

$$r = \delta_{ab}/(\delta_a \delta_b) = \frac{\sum (a_i - \bar{a})(b_i - \bar{b})}{[\sum (a_i - \bar{a})^2 \sum (b_i - \bar{b})^2]^{1/2}} \quad (9)$$

The linear correlation coefficient has the geometric significance of representing the cosine of the angle (Θ) formed between the vectors $[\boldsymbol{a}_i]$ and $[\boldsymbol{b}_i]$.

DNBMP	DNBAP	NH_2	TNFP	C_{18}	PFPh	Phen
−1.626	−1.386	−1.640	−3.045	−3.219	−1.578	−1.386
−1.546	−1.317	−1.314	−2.351	−2.813	−1.745	−1.204
−1.914	−1.253	−1.902	−2.351	−3.219	−1.578	−1.609
−2.031	−1.192	−1.902	−3.045	−3.219	−2.064	−1.897
−1.546	−0.934	−1.497	−1.946	−2.813	−2.197	−1.099
−0.447	0.417	−0.467	−0.742	−2.120	−1.371	−0.916
−0.350	0.609	−0.567	−0.693	−2.120	−1.099	−0.693
−0.397	0.441	−0.567	−0.847	−2.303	−1.008	−0.660
−0.219	0.850	−0.491	−0.480	−2.303	−1.008	−0.539
0.977	1.996	0.440	1.211	−1.514	0.031	0.049
0.945	2.020	0.505	0.795	−1.514	0.076	0.095
0.983	2.136	0.523	1.266	−1.427	0.091	0.182
1.060	2.630	0.540	1.580	−1.514	0.120	0.312
1.109	2.564	0.557	1.580	−1.715	0.188	0.348
0.906	2.234	0.566	1.344	−1.609	0.091	0.236
0.725	2.066	0.440	1.319	−1.609	−0.136	0.125

TABLE IV

LOGARITHM OF CAPACITY FACTORS (LN k') *VERSUS* THE COSINE OF DIHEDRAL ANGLE (DH) FOR BIPHENYL SPECIES ON VARIOUS ELECTRON-ACCEPTOR STATIONARY PHASES

Compound	Cos(DH)	TNFP	TNDBSP	DNBAP	DNPMP	DNAP
Biphenyl	0.775	0.627	−0.150	0.368	0.508	0.604
9,10-Dihydrophenanthrene	0.956	1.251	0.299	0.799	1.092	1.092
Fluorene	1.000	1.679	0.912	1.358	1.405	1.405
Slope [ln k' *vs.* cos(DH)]		4.318	4.070	3.814	3.768	3.309
S.D.		1.012	1.847	1.666	0.624	0.711
y-Intercept		−2.745	−3.351	−2.630	−2.429	−1.978
r^2		0.948	0.829	0.840	0.973	0.956

Another way to compare analytical data that is conveniently in the form of vectors is by calculating the Euclidian distance (D_{ab}):

$$D_{ab} = [\sum(a_i - b_i)^2]^{1/2} = [\boldsymbol{a}_i - \boldsymbol{b}_i][\boldsymbol{a}_i - \boldsymbol{b}_i]^T \quad (10)$$

Massart and Kaufman [47] state that comparison of Euclidian distance calculations is useful in detecting differences in polarity and specificity in liquid stationary phases whereas comparison of linear correlation coefficients detects only specificity, albeit better than Euclidian distance.

Twelve stationary phases were examined using sixteen aromatic hydrocarbons with and without alkyl substituents. These data were collected at a temperature of 25°C using a constant-temperature bath. The linear correlation coefficient and Euclidian distance were calculated for each vector pair (*i.e.*, column of data) in Table III according to eqns. 9 and 10, respectively. The results for the 66 combinations are presented in Table V. To aid in interpreting these data, the combinations were arranged according to some clusters that became apparent through inspection. The group assignments were made as follows: A, $r \geqslant 0.992$ and $D_{ab} \leqslant 3.1$; B, $0.992 > r \geqslant 0.975$ and $3.1 < D_{ab} \leqslant 5.0$; and C, $r < 0.975$ and $D_{ab} > 5.0$. These groups were assigned the more descriptive labels of "close similarity" (A), "some similarity" (B) and "no similarity" (C). As one might expect, the C_{18} phase had little in common with the EA phases, and, under these conditions, C_{18} also differed from the Phen and PFPh phases. It was interesting that NH_2 and TNFP did not have close similarity (*i.e.*, group A) to many of the other EA phases. It was also interesting that the combination with the greatest difference in compensation temperatures (DNBAP–TNDBSP) had a higher group assignment (Group A) than combinations with a smaller difference in compensation temperatures (*e.g.*, DNBMP–TNDBSP in Group B). This is not necessarily in conflict with the entropy–enthalpy compensation data; however, it does suggest that a vector analysis using correlation coefficient and Euclidian distance calculations may be more informative when comparing the subtleties of stationary phases. PFPh, if it behaved as an EA phase at all under these conditions, was not similar to the other EA phases.

The model for EDA chromatography, as described in the Introduction, involves parallel planes between donor and acceptor molecules. As noted previously [18], the lack of planarity in biphenyl (twelve π-electrons) causes it to have a retention time similar to naphthalene (ten π-electrons). To investigate this phenomenon further, the logarithms of the capacity factors (ln k') for biphenyl, 9,10-dihydrophenanthrene and fluorene on several stationary phases were plotted against the cosines of the dihedral angle (cos φ) for the analytes (Table IV). The multi-ring acceptor phases, TNFP and TNDBSP, appeared to have better selection of planar *vs.* non-planar species based on the slope of ln k' *vs.* cos φ. The standard deviations of the slopes and coefficients of determination (r^2) for TNDBSP and DNBAP were large relative to the other EA phases. This may suggest secondary equilibria. Alumina was included with these data because it has been accepted as a useful stationary phase in resolving planar and non-planar analytes. One can see

TNPMP	5-NO_2	DNBMP	Alumina	C_{18}	NH_2	PFPh	Phen
0.389	0.258	−0.058	−0.400	−1.966	0.000	−0.405	−0.244
0.779	0.611	0.264	−0.270	−1.715	0.284	−0.083	0.125
1.071	0.804	0.436	0.131	−1.514	0.339	−0.016	0.080
2.777	2.288	2.074	1.884	1.829	1.525	1.746	0.353
0.722	0.392	0.343	1.356	0.468	0.053	0.044	0.054
−1.781	−1.525	−1.674	−1.894	−3.396	−1.180	−1.758	−0.243
0.937	0.972	0.973	0.659	0.928	0.999	0.999	0.977

that alumina is only mildly effective in that role.

Each stationary phase was also evaluated for its ability to group alkyl-substituted PAHs in narrow bands. In previous studies [11,28] of the grouping behavior of stationary phases, retention indices were used. A model compound is chosen as representing a particular group and all other compounds in the group under study are evaluated in terms of how closely to the model compound they elute. It is not obvious that the collective distance of a series of solutes from a model compound is a better measurement than simply noting the overall width of the

TABLE V

LINEAR CORRELATION COEFFICIENT (r) AND EUCLIDIAN DISTANCE (D_{ab}) CALCULATED FROM THE PAIR OF VECT [LN k' a_1, LN k' a_2, ..., LN k' a_n] AND [LN k' b_1, LN k' b_2, ..., LN k' b_n], WHERE LN k' ϕ_i IS THE LOGARITHM OF THE CAPAC FACTOR OF THE iTH COMPONENT ON STATIONARY PHASE ϕ

The group assignments were made as follows: A, $r \geqslant 0.992$ and $D_{ab} \leqslant 3.1$; B, $0.992 > r \geqslant 0.975$ and $3.1 < D_{ab} \leqslant 5.0$; and C, $r < 0.975$ and I 5.0.

Combination	r	D_{ab}	Group	Combination	r	D_{ab}	Group	Combination	r	D_{ab}	Gr
TNPMP–DNAP	0.998	1.694	A	TNPMP–TNFP	0.991	3.788	B	C_{18}–DNBMP	0.981	8.198	C
TNPMP–DNBMP	0.998	2.708	A	NH_2–DNAP	0.990	2.611	B	C_{18}–DNAP	0.979	9.381	C
5-NO_2–TNPMP	0.997	3.073	A	DNBAP–DNBMP	0.990	4.098	B	C_{18}–TNPMP	0.978	10.88	C
5-NO_2–DNBMP	0.997	0.589	A	DNBAP–TNFP	0.990	4.715	B	C_{18}–5-NO_2	0.978	7.853	C
TNPMP–DNPMP	0.997	1.327	A	5-NO_2–TNDBSP	0.990	3.480	B	Phen–DNPMP	0.976	5.894	C
5-NO_2–DNAP	0.996	1.817	A	DNBMP–TNDBSP	0.989	3.013	B	C_{18}–TNFP	0.974	8.300	C
DNBAP–TNDBSP	0.996	2.414	A	5-NO_2–DNBAP	0.989	4.489	B	Phen–DNAP	0.974	3.576	C
DNAP–TNDBSP	0.996	1.739	A	DNPMP–TNFP	0.988	4.550	B	C_{18}–TNDBSP	0.973	10.60	C
DNAP–DNBAP	0.996	2.913	A	5-NO_2–TNFP	0.988	2.672	B	Phen–DNBAP	0.972	6.052	C
NH_2–DNBMP	0.995	1.299	A	DNBMP–TNFP	0.986	2.389	B	Phen–TNDBSP	0.971	5.187	C
TNPMP–DNBAP	0.995	1.489	A	Phen–DNBMP	0.984	2.272	B	PFPh–TNPMP	0.971	5.495	C
DNAP–DNPMP	0.995	2.747	A	NH_2–TNFP	0.983	3.108	B	PFPh–DNBMP	0.969	2.927	C
TNPMP–TNDBSP	0.995	2.093	A	NH_2–TNDBSP	0.982	4.241	B	C_{18}–DNBAP	0.968	12.23	C
DNAP–DNBMP	0.995	1.386	A	Phen–NH_2	0.982	1.135	B	PFPh–DNAP	0.967	4.176	C
TNDBSP–TNFP	0.994	2.570	A	Phen–TNPMP	0.981	4.634	B	C_{18}–DNPMP	0.967	12.06	C
NH_2–5-NO_2	0.993	0.880	A	Phen–5-NO_2	0.981	1.814	B	PFPh–TNDBSP	0.962	5.659	C
DNPMP–TNDBSP	0.993	2.303	A	Phen–TNFP	0.980	3.938	B	Phen–C_{18}	0.961	6.644	C
DNPMP–DNBAP	0.992	0.745	A	PFPh–5-NO_2	0.975	2.492	B	PFPh–DNBAP	0.959	6.895	C
5-NO_2–DNPMP	0.994	4.301	B	C_{18}–NH_2	0.987	7.168	C	PFPh–NH_2	0.957	1.943	C
NH_2–TNPMP	0.993	3.815	B	NH_2–DNPMP	0.987	5.067	C	PFPh–TNFP	0.953	4.006	C
DNPMP–DNBMP	0.992	3.919	B	NH_2–DNBAP	0.983	5.236	C	Phen–PFPh	0.952	1.561	C
DNAP–TNFP	0.991	2.271	B	PFPh–DNPMP	0.982	6.669	C	PFPh–C_{18}	0.923	5.636	C

TABLE VI

GROUPING OF LN k' VALUES AND COMPARATIVE STATISTICS FOR AROMATIC SOLUTES ON VARIOUS STATIONARY PHASES

No. of π-electrons	Parameter	DNAP	DNPMP	TNPMP	5-NO_2	TNDBSP
6	Mean ln k'	−1.774	−1.193	−1.253	−1.654	−2.055
	Variance	0.019	0.011	0.025	0.037	0.075
	Range	0.368	0.272	0.405	0.442	0.693
	Skewness	0.880	−1.637	−0.432	−2.090	0.614
	Kurtosis	1.013	2.952	−0.541	4.408	−0.831
10	Mean ln k'	−0.136	0.325	0.248	−0.423	−0.063
	Variance	0.006	0.015	0.011	0.002	0.011
	Range	0.186	0.278	0.226	0.091	0.219
	Skewness	−0.512	0.976	0.605	1.635	0.188
	Kurtosis	1.371	−0.063	−2.045	2.513	−4.528
14	Mean ln k'	1.424	2.258	1.774	0.794	1.989
	Variance	0.011	0.034	0.020	0.004	0.078
	Range	0.284	0.431	0.401	0.186	0.814
	Skewness	0.618	0.351	0.555	−0.375	0.501
	Kurtosis	−0.823	−1.765	−0.654	−0.094	−0.607
	Γ (10π − 6π)	1.638	1.518	1.501	1.230	1.993
	Γ (14π − 10π)	1.560	1.933	1.526	1.218	2.052
	$\Gamma \times \Gamma$	2.555	2.934	2.291	1.498	4.089
	Sum of variance	0.036	0.060	0.055	0.043	0.165
	G (Γ)	71.968	48.817	41.392	35.228	24.764

elution range of the group. As the logarithm of capacity factor is proportional to a retention index for a particular group, the same grouping information can be obtained with the former. The selection of which compounds belong to which group is important in comparing the performances of EA phases. The mechanism of EDA chromatography operates primarily on the basis of the number of π-electrons in the donor molecule and secondarily on the planarity of the donor molecule. Therefore, the groups were categorized according to π-electron numbers of six, ten and fourteen. The biphenyls and bridged biphenyls (9,10-dihydrophenanthrene and fluorene) were not included in this evaluation.

In addition to grouping alkyl PAHs in narrow bands, it is important to insure that the bands are well separated from one another. This is important when one is considering switching fractions of HPLC effluent to other techniques such as multi-dimensional HPLC or gas chromatography. A study of grouping behavior was designed to consider practically the stationary phases in terms of grouping and separation. This was accomplished by calculating a single value from the ln k' values of aromatic solutes on each stationary phase.

Within each group on a stationary phase, comparative statistics (mean, variance, range, skewness and kurtosis) were calculated. The grouping aptitude of the EA phases could readily be compared. The mean ln k' for each was used to calculate a value called Γ, the difference in mean ln k' for adjacent groups. The similarity of Γ (group separation number) to α (separation number) can be seen:

$$\alpha = k'_2/k'_1$$
$$\Gamma = \ln k'_2 - \ln k'_1 \quad (11)$$

The best separation would occur when individual Γ values were each at a maximum or when the product of the Γ values was a maximum. Similarly, the best grouping would occur when the combined variance for all groups was at a minimum. These

DNBMP	DNBAP	NH_2	TNFP	C_{18}	PFPh	Phen
−1.733	−1.217	−1.651	−2.548	−3.057	−1.833	−1.439
0.051	0.030	0.066	0.233	0.049	0.081	0.103
0.486	0.452	0.588	1.099	0.405	0.619	0.799
−0.670	1.318	0.251	−0.047	0.609	−0.495	−0.609
−2.374	2.025	−1.841	−2.117	−3.333	−2.460	−0.799
−0.353	0.579	−0.523	−0.690	−2.211	−1.121	−0.702
0.010	0.040	0.003	0.024	0.011	0.029	0.025
0.228	0.433	0.100	0.368	0.182	0.363	0.377
1.067	1.082	0.184	0.972	0.000	−1.657	−0.922
1.206	−0.036	−4.946	1.606	−6.000	2.608	1.788
0.958	2.235	0.510	1.299	−1.558	0.066	0.193
0.015	0.068	0.003	0.071	0.009	0.010	0.013
0.384	0.634	0.126	0.786	0.288	0.323	0.300
−1.018	0.896	−0.634	−1.051	−0.480	−1.424	0.226
1.811	−1.085	−1.343	1.834	0.183	3.121	−1.446
1.379	1.796	1.128	1.857	0.845	0.711	0.737
1.311	1.656	1.033	1.990	0.654	1.187	0.895
1.809	2.973	1.165	3.695	0.553	0.844	0.659
0.076	0.138	0.071	0.328	0.069	0.121	0.141
23.929	21.596	16.352	11.275	7.987	7.007	4.693

opposing performance measures were combined in a single equation to make comparison easier:

$$R_\Gamma = \frac{[\Gamma(10\pi - 6\pi) \times \Gamma(14\pi - 10\pi)]}{[s^2(6\pi) + s^2(10\pi) + s^2(14\pi)]} \qquad (12)$$

The results of these calculations are shown in Table VI. The significance of this new performance parameter (R_Γ or "group resolution") is that it is a single value that combines the effectiveness of a stationary phase to place related solutes into narrow bands and the effectiveness of the stationary phase to maintain separation among the groups. Using the calculated values for R_Γ, the group-resolution effectiveness of the various phases followed the sequence DNAP ≫ DNPMP, TNPMP, 5-NO_2 > TNDBSP, DNBMP, DNBAP > NH_2 > TNFP. PFPh was ranked with C_{18} and Phen.

In summary, the entropy–enthalpy compensation technique was not very helpful in providing comparisons among the various electron-acceptor phases. The vector-analysis techniques of linear correlation coefficient calculation and Euclidian distance calculation provided two quantitative measures for comparing stationary phases that were much more useful. As the most effective application of electron-acceptor phases is group separation, the parameter R_Γ (group resolution) should be helpful in evaluating these electron-acceptor phases and those to come. It has been shown that electron-acceptor phases are also effective at separating bridged-biphenyl compounds based on dihedral angle. With this added understanding, new applications of these curious stationary phases may emerge.

By applying the comparison techniques described here, it was found that DNAP was better at grouping aromatic solutes than DNPMP (R_Γ 72 and 49, respectively). Conversely, DNPMP was found to be slightly better than DNAP at separating species based on dihedral angle (slope in Table V 3.8 and 3.3, respectively).

ACKNOWLEDGEMENT

We thank S. C. Johnson and Son, Inc. (Racine, WI, USA) for financial support and the loan of equipment.

REFERENCES

1 W. Holstein and H. Hemetsberger, *Chromatographia*, 15 (1982) 251.
2 C. H. Lochmüller and C. W. Amoss, *J. Chromatogr.*, 108 (1975) 85.
3 C. H. Lochmüller, R. R. Ryall and C. W. Amoss, *J. Chromatogr.*, 178 (1979) 298.
4 H. Hemetsberger, H. Klar and H. Ricken, *Chromatographia*, 13 (1980) 277.
5 W. E. Hammers, A. G. M. Theeuwes, W. K. Brederode and C. L. Delingny, *J. Chromatogr.*, 234 (1982) 321.
6 P. L. Grizzle and J. S. Thomson, *Anal. Chem.*, 54 (1982) 1071.
7 E. P. Lankmayr and K. Müller, *J. Chromatogr.*, 155 (1978) 139.
8 L. Nondek and J. Málek, *J. Chromatogr.*, 155 (1978) 187.
9 L. Nondek, M. Minárik and J. Málek, *J. Chromatogr.*, 178 (1979) 427.
10 L. Nondek and R. Ponec, *J. Chromatogr.*, 294 (1984) 175.
11 J. S. Thomson and J. W. Reynolds, *Anal. Chem.*, 56 (1984) 2434.
12 L. Nondek and M. Minárik, *J. Chromatogr.*, 324 (1985) 261.
13 S. A. Matlin, J. S. Tinker, A. Tito-Lloret, W. J. Lough, L. Chan and D. Bryan, *Proc. Anal. Div. Chem. Soc.*, 16 (1979) 354.
14 S. A. Matlin, W. J. Lough and D. G. Bryan, *J. High Resolut. Chromatogr. Chromatogr. Commun.*, 3 (1980) 33.
15 G. Eppert and T. Schinke, *J. Chromatogr.*, 260 (1983) 305.
16 G. Félix and C. Bertrand, *J. High Resolut. Chromatogr. Chromatogr. Commun.*, 7 (1984) 160.
17 G. Félix and C. Bertrand, *J. High Resolut. Chromatogr. Chromatogr. Commun.*, 7 (1984) 714.
18 K. J. Welch and N. E. Hoffman, *J. High Resolut. Chromatogr. Chromatogr. Commun.*, 9 (1986) 417.
19 R. S. Mulliken and W. B. Person, *Molecular Complexes*, Wiley-Interscience, New York, 1969, p. 448.
20 S. C. Wallwork, *J. Chem. Soc.*, (1961) 494.
21 L. R. Snyder, *Principles of Adsorption Chromatography*, Marcel Dekker, New York, 1968.
22 L. R. Snyder, in Cs. Horváth (Editor), *High Performance Liquid Chromatography*, Vol. 3, Academic Press, New York, 1963, p. 157.
23 L. R. Snyder, *LC Mag.*, 1 (1983) 478.
24 R. P. W. Scott, *J. Chromatogr.*, 122 (1976) 35.
25 L. Nondek, P. Dienstbier and R. Rericha, *J. High Resolut. Chromatogr. Chromatogr. Commun.*, 11 (1988) 217.
26 L. R. Snyder, *J. Phys. Chem.*, 67 (1963) 240.
27 L. R. Snyder, *J. Chromatogr.*, 25 (1966) 274.
28 M. Popl, V. Dolonsky and J. Mostecky, *J. Chromatogr.*, 91 (1974) 649.
29 W. Melander, D. E. Campbell and Cs. Horváth, *J. Chromatogr.*, 158 (1978) 215.
30 K. Jinno and N. Ozaki, *J. Liq. Chromatogr.*, 7 (1984) 877.
31 R. J. Laub and S. J. Madden, *J. Liq. Chromatogr.*, 8 (1985) 187.
32 K. Jinno, T. Ohshima and Y. Hirata, *J. High Resolut. Chromatogr. Chromatogr. Commun.*, 5 (1982) 621.
33 C. M. Riley, E. Tomlinson and T. L. Hakenscheid, *J. Chromatogr.*, 218 (1981) 427.
34 H. Colin, J. C. Díez-Masa, G. Guiochon, T. Czajkowska and I. Miedziak, *J. Chromatogr.*, 167 (1978) 41.
35 K. Jinno and Y. Hirata, *J. High Resolut. Chromatogr. Chromatogr. Commun.*, 5 (1982) 621.
36 C. A. Chang, C.-F. Tu and C.-S. Huang, *J. Chromatogr. Sci.*, 22 (1984) 321.
37 M. Kuchar, E. Draus, V. Rejholec and V. Miller, *J. Chromatogr.*, 449 (1988) 391.
38 H. Issaq and M. Jaroniec, *J. Liq. Chromatogr.*, 12 (1989) 2067.
39 K. J. Laidler, *Trans. Faraday Soc.*, 55 (1959) 1725.
40 R. Lumry and S. Rajender, *Biopolymers*, 9 (1970) 1125.
41 H. E. Baumgarten, *Org. Synth.*, 5 (1973) 1029.
42 S. A. Nabi, S. Haque and P. M. Qureshi, *Talanta*, 30 (1983) 989.
43 J. Sedlácek and L. Nondek, *J. High Resolut. Chromatogr. Chromatogr. Commun.*, 8 (1985) 364.
44 R. R. Krug, W. G. Hunter and R. A. Grieger, *J. Phys. Chem.*, 80 (1976) 2335.
45 R. R. Krug, W. G. Hunter and R. A. Grieger, *J. Phys. Chem.*, 80 (1976) 2341.
46 W. Melander, J. Stoveken and Cs. Horváth, *J. Chromatogr.*, 199 (1980) 35.
47 D. L. Massart and L. Kaufman, *The Interpretation of Analytical Chemical Data by the Use of Cluster Analysis*, Wiley, New York, 1983, p. 15.